Biomass Conversion and Biorefinery (2024) 14:22125–22136
https://doi.org/10.1007/s13399-023-04343-1

ORIGINAL ARTICLE

Plausible antioxidant and anticonvulsant potential of brain targeted naringenin-conjugated graphene oxide nanoparticles

Raghul Murugan[1] · G. Mukesh[1] · B. Haridevamuthu[1] · P. Snega Priya[1] · Raman Pachaiappan[2] · Bader O. Almutairi[3] · Selvaraj Arokiyaraj[4] · Ajay Guru[5] · Jesu Arockiaraj[1]

Received: 21 February 2023 / Revised: 5 May 2023 / Accepted: 13 May 2023 / Published online: 22 May 2023

Abstract

Epilepsy is a condition in the brain cause frequent seizures and related comorbidities. The major hindrance during the design of antiepileptic drugs is their permeability through the blood–brain barrier (BBB). Recently, advancements in biology and engineering have led to the development of nanocomposites for drug delivery through the BBB. In this study, we have fabricated a novel type of nanoparticles using a plant compound, naringenin, with graphene oxide (NGO). The mean size of the fabricated nanoparticles was obtained as 73.1 nm and the polydispersity value was obtained as 3.286 through dynamic light scattering measurement. The average zeta potential value, − 49.6 mV, showed that the nanoparticles were strongly anionic in nature. A fluorescent imaging experiment demonstrated that the fabricated fluorescein isothiocyanice (FITC) tagged NGO nanoparticles localised successfully in adult zebrafish brains. The in vitro antioxidant assay showed that NGO nanoparticles have reduced the levels of 2,2-diphenyl-1-picrylhydrazyl (DPPH) and 2,2′-azino-bis(3-ethylbenzothiazoline-6-sulfonic acid) (ABTS) free radicals upto 41.5 ± 0.51 and 64.25 ± 1.62%, respectively. In vivo developmental toxicity assessment indicated that NGO nanoparticles were non-toxic to the developing embryo of zebrafish. The percentage of ROS and apoptosis in zebrafish larvae due to pentylenetetrazole (PTZ) exposure was significantly reduced by NGO pre-treatment. Additionally, the behavioural analysis showed that NGO could suppress the PTZ-induced convulsant behaviour in adult zebrafish. From the results of both in vitro and in vivo experiments, we concluded that NGO nanoparticles could be used as promising medicine to treat free radical-induced neuronal damage and epilepsy, provided the results need to be reconfirmed in the mammalian model as well as a clinical trial.

Keywords Epilepsy · Antioxidant · Brain · Naringenin · Nanoparticles · Zebrafish

1 Introduction

Epilepsy is a chronic neurological disorder characterised by a persistent propensity to produce seizures. Reports state that the occurrence of epilepsy among the world population is over 70 million. People with epilepsy suffer from recurrent seizures, seizure-related comorbidities, stigma, and disability [1]. Even though certain nations have access to highly advanced treatment, in nations with low resources, up to 90% of epileptic patients do not receive proper care or antiepileptic medicine in the usual sense [2]. Numerous pathophysiological processes, including neurotransmitter changes, oxidative stress and an imbalance between the Glutamatergic and GABAergic systems, have been postulated

✉ Ajay Guru
ajayguru.sdc@saveetha.com

✉ Jesu Arockiaraj
jesuaroa@srmist.edu.in

[1] Toxicology and Pharmacology Laboratory, Department of Biotechnology, Faculty of Science and Humanities, SRM Institute of Science and Technology, Chengalpattu District, Kattankulathur 603203, Tamil Nadu, India

[2] Department of Biotechnology, School of Bioengineering, Faculty of Engineering and Technology, SRM Institute of Science and Technology, Chengalpattu District, Kattankulathur 603203, Tamil Nadu, India

[3] Department of Zoology, College of Science, King Saud University, P.O. Box 2455, Riyadh 11451, Riyadh, Saudi Arabia

[4] Department of Food Science & Biotechnology, Sejong University, Seoul 05006, Korea

[5] Department of Conservative Dentistry and Endodontics, Saveetha Dental College and Hospitals, SIMATS, Chennai 600 077, Tamil Nadu, India

to underlie epilepsy. The antiepileptic medications that are clinically available and used to treat epileptic seizures cause several psychological comorbidities. Hence, the need for new antiepileptic medications with better tolerance and efficacy remains unmet [3].

As said earlier, one of the factors involved in the onset of epilepsy is oxidative stress due to the generation of free radicals. Free radicals such as reactive oxygen species (ROS) and reactive nitrogen species (RNS) are significant factors involved in the aetiology of epilepsy [4]. Excess production of free radicals during neuroinflammation damages neurons and cause neurodegenerative disease such as epilepsy [5]. On the other hand, through voltage-gated and N-methyl-d-aspartate (NMDA)-dependent ion channels, epileptic seizures enhance the inflow of Calcium (Ca^{2+}). Once the NMDA type of glutamatergic receptor is activated, it triggers the Ca-dependent Nitric oxide synthetase (NOS) activity and nitric oxide (NO) release [5]. Hippocampus astrocytes, oxidative stress, and neuron death are pathogenic and biochemical phenomena connected to epilepsy that are facilitated by NR2B subunits of the NMDA receptor [6]. The NO produced reacts with ROS and forms nitroxyl radicals, which further leads to neuronal damage. Previous reports indicated elevated NO levels during epilepsy in animal models [7]. Pentylenetetrazole (PTZ) induced kindling of seizures is a well-established model to study chronic epilepsy. The mechanism of PTZ involves molecular alterations that induce oxidative stress and subsequent neurodegeneration. Several studies report that PTZ kindling induces oxidative damage in mice [8]. The brain is highly prone to damage by free radicals since the action of antioxidant enzymes is highly limited. Hence, we hypothesise using external free radical scavengers to remedy oxidative stress-induced neuronal damage during epileptogenesis.

Flavonoids are among the naturally occurring substances that can alter various signalling pathways implicated in neurodegeneration [9]. One of those naturally occurring flavonoids with neuroprotective properties is naringenin (NA). Growing attention has been given in recent years to NA for its possible therapeutic benefits on neurological illnesses [10]. NA has shown promise in treating neurodegenerative diseases, but its limited bioavailability and demanding access to the brain present significant obstacles. The blood–brain barrier (BBB), one of the body's most critical microenvironments, protects the central nervous system and controls its homeostasis. BBB is a highly intricate system that tightly controls the transit of ions, a small number of tiny molecules, and an even smaller number of macromolecules from the blood to the brain, shielding it from harm and disease. However, BBB also severely hinders medicine delivery to the brain, making it impossible to treat various neurological illnesses [11]. As a result, a number of ways are being studied to improve medicine delivery across the BBB. The use of nanoparticles in various technologies is growing quickly. Nanoparticles are particles with a size between 1 and 100 nm that function as a single entity for transportation and characteristics. These engineered customisable devices with sizes in the order of nanometres have recently been suggested as an attractive tool, perhaps capable of solving the unmet problem of increasing medication transport across the BBB [12]. Among different nanostructures, graphene-based nanostructures, particularly those made from reduced graphene oxide, are finding greater application in neuronostics. For instance, surface-enhanced Raman spectroscopy has been utilised to identify beta-amyloid and tau proteins in whole blood using hybrid nanostructures made of graphene oxide (GO) and magnetic core-plasmonic shell nanoparticles [13]. Graphene-based platforms may be helpful for the treatment of Alzheimer's disease, Parkinson's disease, and amyotrophic lateral sclerosis [14]. Reduced GO (rGO) has been utilised to detect the neurotransmitter dopamine [15]. Graphene has been employed as a scaffold to restore lost functioning in brain cells in addition to these diagnostic and therapeutic uses [16]. In this study, we prepared nanoparticles fabricated with NA and GO to examine their drug delivery potential across the BBB of zebrafish. We have also evaluated the antioxidant and anticonvulsant effects of fabricated nanoparticles in PTZ-exposed larval and adult zebrafish.

2 Materials and methods

2.1 Reagents

Naringenin (NA, molecular weight-272.257 g/mol, purity-95%, purchased from Sigma-Aldrich), NA stock solution (1 mM) was prepared by dissolving in NA in 1 × PBS (pH-7.4), Pentylenetetrazole (PTZ, purity 99%, purchased from SRL), reduced graphene oxide (rGO, purchased from Sigma-Aldrich). 2,2-Diphenyl-1-Picrylhydrazyl (DPPH, purity-95%), 2,7-Dichlorofluorescein Diacetate (DCFDA, purity-97%), Acridine orange (AO, purity-99%), Fluorescein Isothiocyanate Isomer I (FITC, purity-95%) were purchased from SRL Pvt. Ltd, ABTS salt (purity-98.5%, purchased from SRL Pvt. Ltd), Potassium persulfate (purity-98%, SRL Pvt. Ltd).

2.2 Fabrication of NGO nanoparticle reagents

Naringenin-graphene oxide (NGO) nanoparticles were prepared as previously described [17] with a few minor changes. The rGO was dispersed in deionised water to obtain GO solution (0.5%). Then, the mixture was vortexed well to obtain a homogenous suspension. To achieve the desired final concentration, 1 mM NA in PBS was combined with GO solution. Then, the solution was subjected to ultrasonication using a probe Sonicator (Vibracell, Sonics material Inc., Newtown, CT) for 60 min with 5-min on/off cycles. The procedure was repeated to obtain enough nanoparticle that was needed for all the experiments.

The free NA in NGO solution was filtered using 30 KDa filter and the concentration of NA in NGO was determined using UV spectrometer at 256 nm as described by [18]. The percentage of drug loaded in nanoparticle was calculated using the following equation.

Drug loaded (%) = ((OD of NA—OD of untrapped NA)/OD of nanoformulation) × 100.

The conjugated NGO nanoparticles were redispersed in distilled water and taken for further characterisation. The dilution of NGO stock was carried as 20, 40, 60, 80 and 100 µL per 1 mL of PBS, to achieve the final concentration of NA in the NGO as 20, 40, 60, 80 and 100 µM, respectively.

2.3 Physiochemical, morphological and functional group characterisation for NGO

The particle size, polydispersity index (PI) and zeta potential of the prepared NGO were analysed using the zeta analyser (Horiba Scientific SZ-100). The NGO solution of 100 µL mixed with 2 mL deionised water as a dispersion medium of viscosity 0.893 mPa.s at 25.1 °C. To picture surface morphology, the synthesised NGO solution was dried into thin film over silica substrate using a hot plate and the substrate was mounted was visualised under high-resolution scanning electron microscopy (HRSEM) (Thermoscientific Apreo S). The size distribution of individual nanoparticle was calculated in images from HRSEM using ImageJ software [19]. Additionally, the functional groups in NGO solution were determined using Fourier-transform infrared (FTIR) spectroscopy (Shimadzu) analysis with the wave number ranging from 400 to 4000 cm^{-1}. The crystallographic structure of NGO was examined using X-ray diffraction (XRD) (BRUKER USA D8 Advance, Davinci, Germany) from a range (2θ) of 5° to 60°.

2.4 In vitro *drug release assay*

The in vitro drug release assay which mimics the oral drug administration was performed using Dialysis membrane suspended in solutions of physiological pH-1.2 (HCl) and 6.8 (PBS) [18]. The NGO solution (100 µM) was taken in dialysis membrane (Repligen, MA, US) suspended in the medium and was kept in shaker incubator of 100 rpm at 37 °C. The free molecules of NA released through the 0.2-µm pores of filter membrane were collected at different time intervals (24, 48, 72 and 96 h) and quantified using UV–visible spectrophotometer at 288 nm.

2.5 In vitro *screening of antioxidants potential of NGO*

To determine in vitro antioxidant potential of NA, GO and NGO, the stock solutions were prepared as 1 mM Trolox, 1 mM NA, and NGO solution (stock preparation explained in Sect. 2.1). From the stock, the working solution is prepared as group A (20 µM), group B (40 µM), group C (60 µM), group D (80 µM) and group E (100 µM). For GO, 0.5% solution was prepared as stock and diluted as same as NGO solution.

2.5.1 DPPH scavenging assay

The DPPH radical scavenging activity of NGO was performed as described with some modifications [20]. DPPH solution (300 µM) was mixed with different volumes of Trolox, NA, GO and NGO and incubated in the dark for 30 min. After incubation, the samples were taken for quantification at 517 nm wavelength using UV–visible spectrometer (Shimadzu-UB1800) and expressed in percentage of inhibition.

2.5.2 *$ABTS^+$ cation scavenging assay*

The ABTS cation radicals decolourisation test was slightly modified to assess the compound's (NA, GO, NGO) capacity to scavenge free radicals [21]. Briefly, ABTS solution was prepared by dissolving ABTS salt (7.0 mM) in potassium persulfate (2.45 mM). The reaction mixture was diluted with 0.2 M PBS (pH 7.4) at 30 °C to an absorbance of 0.7 ± 0.02 at 734 nm. NA, GO, and NGO was mixed in varying volumes and maintained at 30 °C for one hour. The proportion of ABTS radical scavenging activity was determined using data obtained at 734 nm.

2.6 NO scavenging assay

A previously published Griess reagent method was followed with a few minor modifications for the NO scavenging activity [22]. Freshly prepared 0.1% naphthyl ethylene diamine dihydrochloride in 2.5% phosphoric acid was mixed with 1% sulphanilamide in 2.5% phosphoric acid to form the Griess reagent. The NA, GO, and NGO were each combined with a different concentration of Sodium nitroprusside (10 mM) in 1X PBS, and the Griess reagent was added in an equal amount. The absorbance was measured at 546 nm following incubation, and the percentage of nitric oxide inhibition was calculated.

2.7 Zebrafish maintenance and treatment

Zebrafish larvae and adults were purchased from Tharun fish farm, Chennai, and were maintained as per the regulations of institutional ethical committee approval (SAF/IAEC/211215/004). For zebrafish larvae and adult fish, the experimental groups were divided as control (untreated healthy fish), PTZ (exposed to 15 mM PTZ), NA (100 µM

NA + 15 mM PTZ), GO (0.5% GO + 15 mM PTZ) and NGO (100 µM + 15 mM PTZ). Zebrafish larvae (96 hpf) cultured in E3 were pre-treated with NA, GO and NGO, respectively in NA, GO and NGO groups. After 24 h of pre-treatment, larvae in each group (except the control group) were exposed to PTZ (15 mM) containing E3 medium for 1 h and then taken for further analysis. For adult fish, 10 µL from each stock solution was injected using microinjection (Thermoscientific, USA), six hours before the PTZ exposure. Then the fish were exposed to 15 mM PTZ solution and taken for further analysis.

2.8 Developmental toxicity assessment

Zebrafish embryos (3 hpf) were used to determine the developmental toxicity of NA, GO and NGO. Zebrafish embryo was taken in 6-well plates and various volume of NA, GO and NGO was added in wells and a photograph of the embryos was taken every 24 h until 3 days. Mortality among embryos was calculated and plotted in the graph using GraphPad Prism 4 software [23].

2.9 *Determination of* in vivo *ROS reducing the potential of NGO*

To assess the impact of NA, GO, and NGO on in vivo ROS scavenging, DCFDA fluorescent staining assay was carried out in 96 hpf zebrafish larvae. Zebrafish larvae pre-treated with NA, GO and NGO were exposed to PTZ for 1 h. Then the larvae were anesthetised using 0.01% tricaine, stained with 20 µg/mL of DCFDA and taken for imaging under fluorescent microscopy (Leica microsystems, Wetzlar and Mannheim, Germany). The fluorescence intensity emitted from the zebrafish larvae was quantified using ImageJ software [24].

2.10 *Determination of* in vivo *apoptosis level in zebrafish larvae*

The zebrafish larvae were stained with A.O. to determine the onset of apoptosis. Zebrafish larvae (96 hpf) from each group were anaesthetised with 0.01% tricaine (Sigma-Aldrich) and stained with AO of concentration 20 µg/ml. After adding the stain, larvae were kept in the dark for 20 min, followed by washing with 1 × PBS. Larvae were then taken in glass slides and observed under the fluorescent microscope. The percentage of apoptosis was calculated by measuring the fluorescence intensity using ImageJ software [25].

2.11 Localisation of NGO in larvae and adult zebrafish

NGO solution (100 µg/mL) was mixed with 50 µM of FITC and incubated overnight. Then the mixture was centrifuged thrice at 12000 rpm for 15 min, and the pellet was dissolved in freshwater [26]. The FITC-NGO mixture prepared was injected into adult zebrafish using microinjection. After 6 h, the brain from the zebrafish was separated and fixed using 4% formaldehyde for 24 h. Then the brain was sectioned using the Cryostat microtome (Leica CM1520) and the sections were observed under the fluorescent microscope.

2.12 Zebrafish behavioural analysis

The changes in the behavioural pattern of adult zebrafish were determined by novel tank assay. The zebrafish were injected with NGO of 10 µL through microinjection. After 6 h, the injected zebrafish were introduced to the PTZ solution for 5 min. Then the zebrafish were transferred to novel tank water and the behaviour was recorded. The movement of zebrafish was processed using UMATracker software [27] and plotted in Origin software.

2.13 Statistics

The data presented in this study are the mean of three replicates and their respective standard deviation (S.D.). Also, the data in graphs were analysed using one-way ANOVA and two-way ANOVA followed by Dunnet, Bonferronni and Tukey multiple comparisons using GraphPad Prism (version 9.0).

3 Results and discussion

3.1 Characteristics of NGO

Generally, the size of nanoparticles should be between 1 and 100 nm [28]. In this study, the results obtained from the zeta analyser showed that the mean (Z-average) particle diameter of fabricated NGO nanoparticles was 73.1 nm, whereas the PI was obtained as 3.286. The charge and potential stability of the particle in a medium were determined in terms of zeta potential. The zeta potential value greater than + 30 mV and less than -30 mV, indicates the strong cationic and anionic nature of the nanoparticles, respectively. In this study, the mean zeta potential obtained for NGO was -49.6 mV which represents strong anionic nature of fabricated NGO. The drug loading capacity in nanoparticle was determined by indirect method using UV visible spectrometer analysis and the results obtained showed that 89.37% of NA was conjugated with GO in NGO nanoparticles. Additionally, to study the morphological characteristics, NGO was pictured under HRSEM and resultant images were shown in the Fig. 1. The morphology of NGO observed under HRSEM at the magnification of 1×10^5X showed the formation of spikes-containing elliptical particles.

Further, the size distribution of nanoparticle from SEM calculated using ImageJ software showed that the length and width of particle were 27.99 and 16.35 respectively. The structure of nanoparticles observed in SEM was further studied using XRD pattern analysis. The result from the XRD analysis was plotted and presented in Fig. 1. The resultant pattern from XRD analysis for NGO nanoparticles showed diffraction peaks at angles 25.3°, 26.3°, 28.1°, 32.7°, 38.5°, 40.1°, 43.3° and 54.4° corresponds to (111), (002), (220), (101), (111), (111), (111) and (110) planes respectively. The diffraction angles such as 28.9, 32.7, 38.5, 54.4 indicates belong to graphene oxide as reported previously [18, 29]. FTIR analysis was carried out to determine the functional groups present in NGO nanoparticles, whereas the plane (002) at angle 25.3° indicates NA as previously reported by Krishnakumar el al [30]. The graphical representation of FTIR results is displayed in Fig. 1. A peak was observed at 3323 cm^{-1}, which represents the O–H stretch. Another peak was observed at wavelength of 1637, which suggests the C = O stretch. Both these peaks were common in NA, GO and NGO. Whereas, in the fingerprint region, NGO showed a short peak at wavelength 1016, representing the C-H stretch [31].

3.2 Drug release assay

The results from the drug release assay (Fig. 2) showed that at pH 1.2, the percentage of drug released was 0.67 ± 0.5, 18.23 ± 3.13, 39.24 ± 3.36, 55.19 ± 2.28 and 68.87 ± 6.47 at 0, 24, 48, 72 and 96 h respectively. Whereas in pH 6.8, the percentage of drug release at intervals 0, 24, 48, 72 and 96 h was 0.45 ± 0.25, 13.64 ± 3.90, 29.1 ± 3.63, 45.19 ± 4.22 and 59.61 ± 2.03 respectively. The cumulative percentage of drug released at pH 1.2 was less compared to drug release at pH 6.8. The earlier literature states that the contraction in nanoformulation occurs at acidic pH due to the unionisation of carboxylic acids, which leads to a slower rate of drug release [32]. However, a comparatively higher percentage of degradation was observed at pH 6.8 which shows that the prepared nanoparticle was pH sensitive and could aid in the sustained release of NA in the stomach and intestinal environment.

3.3 Free radicals scavenging activity of NGO

The exact mechanisms of antioxidant molecules are difficult to study using in vivo methods. Hence, there are few cell-free assays to study the chemical mechanism of action of the antioxidant compound. The two significant mechanisms

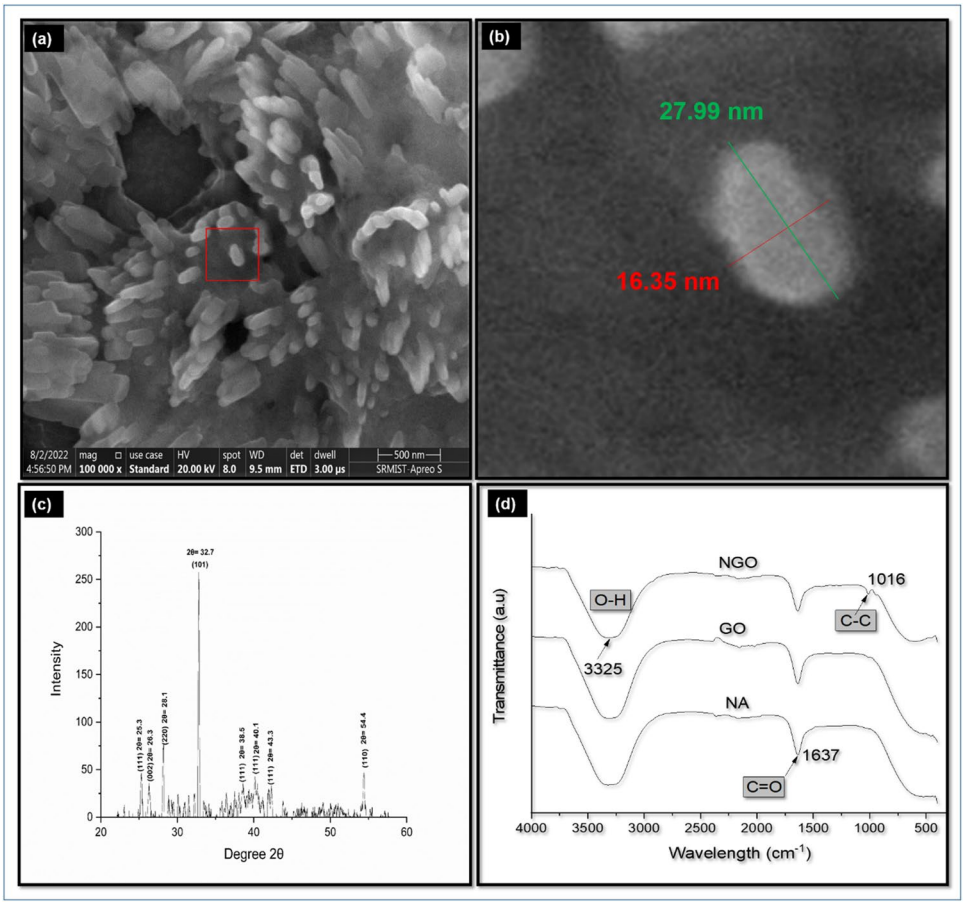

Fig. 1 Morphology analysis of Naringenin-graphene oxide (NGO) nanoparticles. (**a**) Spike structures (highlighted in red) of NGO nanoparticles observed under a scanning electron microscope (HRSEM), scale- 500 nm, (**b**) individual NGO nanoparticle (highlighted in Fig. 1a), which size was calculated using ImageJ software, (**c**) XRD patterns of fabricated NGO nanoparticle. The diffraction peaks at 2θ values of 25.3°, 26.3°, 28.1°, 32.7°, 38.5°, 40.1°, 43.3° and 54.4° correspond to (111), (002), (220), (101), (111), (111), (111) and (110) planes respectively were obtained from NGO nanoparticle. (**d**) FTIR spectra of obtained from NA, GO, NGO nanoparticle. The peak at 3323 and 1637 cm^{-1} corresponds to O–H and C = O were observed in all three samples, whereas in NGO nanoparticle, a peak at 1016 which corresponds to C–C stretch was observed

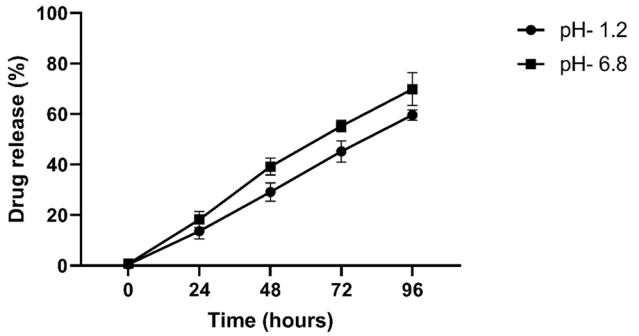

Fig. 2 The percentage of drug released from the fabricated nanoparticle at different physiological pH such as 1.2 and 6.8 which resembles stomach and intestinal release. The drugs released from dialysis membrane at different time intervals (0, 24, 48, 72 and 96 h) were converted into percentages and the graph was plotted with mean ± S.D

such as hydrogen atom transfer (HAT) and single electron transfer (SET) are involved in free radical scavenging due to antioxidant molecules. DPPH and ABTS are the most common methods used to determine the HAT and SET mechanisms of antioxidants. The change of colour of DPPH from dark violet to pale due to the antioxidant action of NA, GO and NGO was quantified using a UV–visible spectrophotometer. The percentage of DPPH radicals scavenged by Trolox was 79.15 ± 10.34. Whereas NA, GO and NGO showed a concentration-dependent increase in DPPH radical scavenging activity with respective values of 24.95 ± 0.35%, 18.1 ± 0.2%, and 41.5 ± 0.51% in group E (Fig. 3). The ABTS cation scavenging assay was used to determine the antioxidant potential NA, GO and NGO in the presence of peroxides. The result obtained by U.V.- spectrophotometer analysis showed that NA, GO and NGO reduced ABTS cation up to 46.5 ± 2.89, 32.8 ± 1.06, and 64.25 ± 1.62% in group E, respectively (Fig. 3). The results obtained from nitric oxide assay showed that at group E, the percentage of free nitric oxide molecules present after addition of NA, GO and NGO were reduced in a concentration-dependent manner and showed 30.1 ± 0.9%, 16.5 ± 2.61% and 24.2 ± 1.4%, respectively in group E (Fig. 3).

The result from the current study indicates that NGO nanoparticles showed DPPH radical scavenging activity in a concentration-dependent manner. While compared with NA and GO, NGO showed higher scavenging of DPPH radicals. Similarly, in the ABTS assay, NGO nanoparticles showed higher scavenging of ABTS radicals compared to NA and GO Additionally, the increase in scavenging of ABTS by NGO nanoparticles showed a concentration-dependent manner. Both these results indicate that NGO has the potential to scavenge the free radicals by donating hydrogen or by transferring one or more electrons [33]. Furthermore, the results from the NO estimation method showed that the level of nitric oxide in

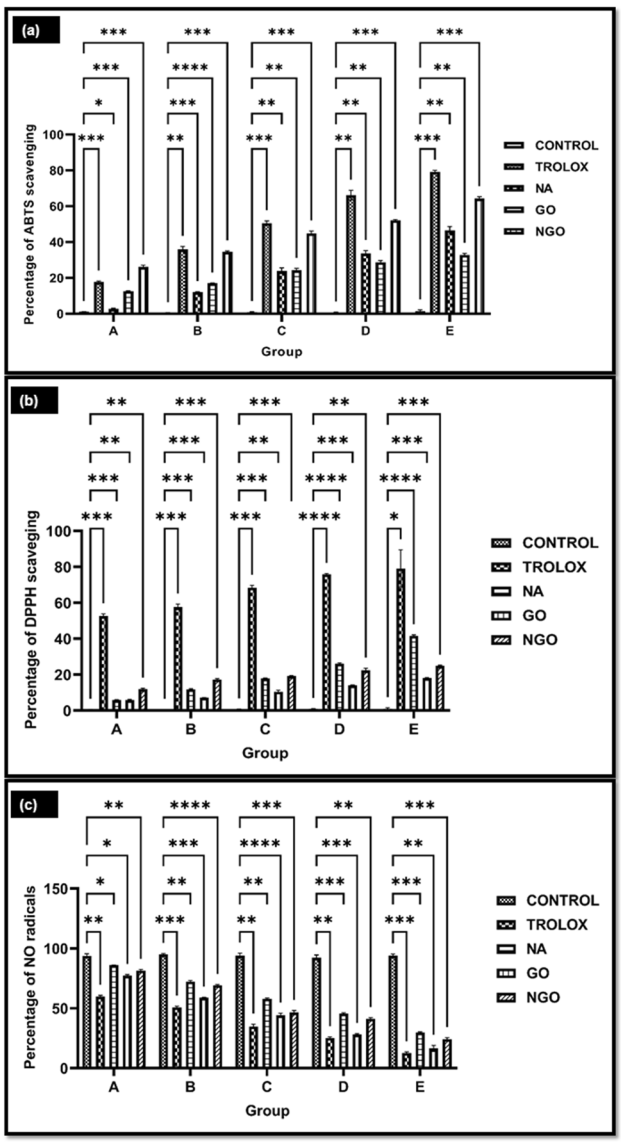

Fig. 3 In vitro antioxidant assays (**a**) ABTS.$^{+}$ scavenging assay, (**b**) DPPH radical scavenging assay, (**c**) nitric oxide radicals scavenging assay. PBS (1X) was taken as control. Group A (20 µM), group B (40 µM), group C (60 µM), group D (80 µM) and group E (100 µM) were aliquots from 1 mM stock of Trolox, NA, NGO nanoparticle and 0.5% GO solution. The graph is plotted with data from triplicates of experiments using two-way ANOVA analysis followed by the Dunnett multiple comparison method. * represents significant difference $p < 0.05$, ** represents significant difference $p < 0.01$, *** represents significant difference $p < 0.001$ and **** represents significant difference $p < 0.0001$

the solution was reduced in a concentration-dependent manner with the addition of NA, GO and NGO. Scavenging of NO radicals subsequently reduces the generation of nitroxyl radicals, as discussed earlier. Although the antioxidant mechanism of NA was well studied earlier, the results from our experiment showed that the antioxidant scavenging potential of NA was enhanced through the formulation of NGO.

3.4 Effect of NGO on zebrafish embryo development

Zebrafish embryos were used in the study to demonstrate the antioxidant and antiepileptic activity of fabricated NGO in the in vivo vertebrate model. The results from the zebrafish embryo developmental toxicity assessment showed no malformation in NA and NGO-treated embryos (Fig. 4). Whereas, in GO pre-treated group, morphological malformation was observed at the end of day 3. The mortality results showed that at the end of day 3, the number of larvae that survived in NA and NGO was 17 ± 1 and 18 ± 1, respectively. Whereas in the GO group, the number of larvae that survived at the end of day 3 was 14 ± 2. The results from the developmental toxicity assay indicate that both NA and NGO were non-toxic to developing zebrafish embryos. These results are similar to an earlier finding [34], which states that the anionic nanoparticles are non-toxic at lower concentrations and the level of toxicity exerted by anionic nanoparticles is less compared with neutral and cationic nanoparticles. On the contrary, the embryo treated with GO showed morphological abnormality at 3 dpf (bent spine). A similar result was also reported previously on GO-induced toxicity in zebrafish embryos [35]. Additionally, the mortality analysis indicates that there is no significant difference between NGO and control groups (Fig. 3). But a considerable number of mortality differences among embryos was observed between the control and GO groups at the end of 3dpf. Both the results from developmental toxicity and mortality analysis proved that

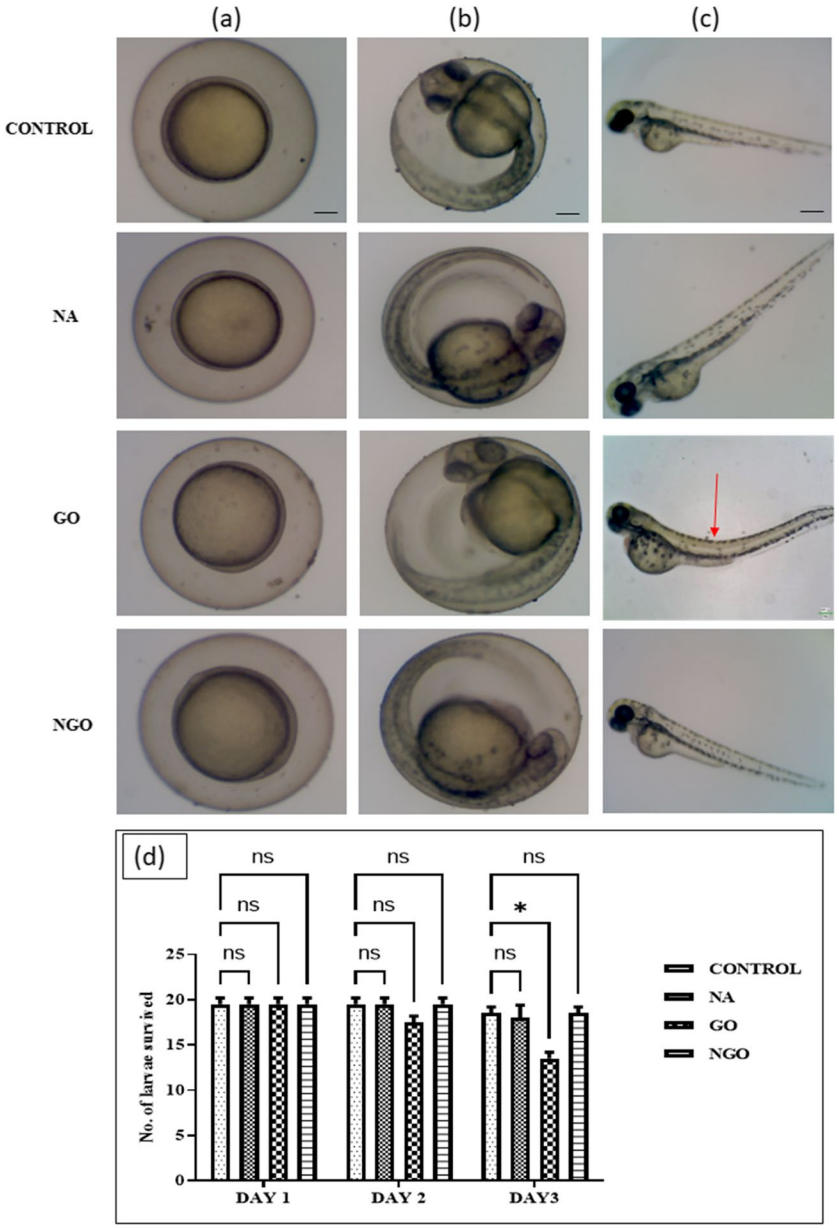

Fig. 4 Zebrafish embryo developmental toxicity assay. Zebrafish embryos after treatment with PBS (control), NA, GO and NGO nanoparticles were observed under a light microscope for 3 consecutive days. (**a**) Gastula stage of the embryo on day 1, (**b**) after organogenesis on day 2, (**c**) larval stage (hatched from an embryo) on day 3; arrow indicates the bent spine observed in GO-treated larvae; scale = 200 µm. (**d**) The number of larvae that survived up to 3 days in the control, NA, GO and NGO groups was recorded and data in the graph represent mean and SD calculated from three independent experiments. * represents a significant difference at $p < 0.05$ calculated using two-way anova following Tukey multiple comparison method

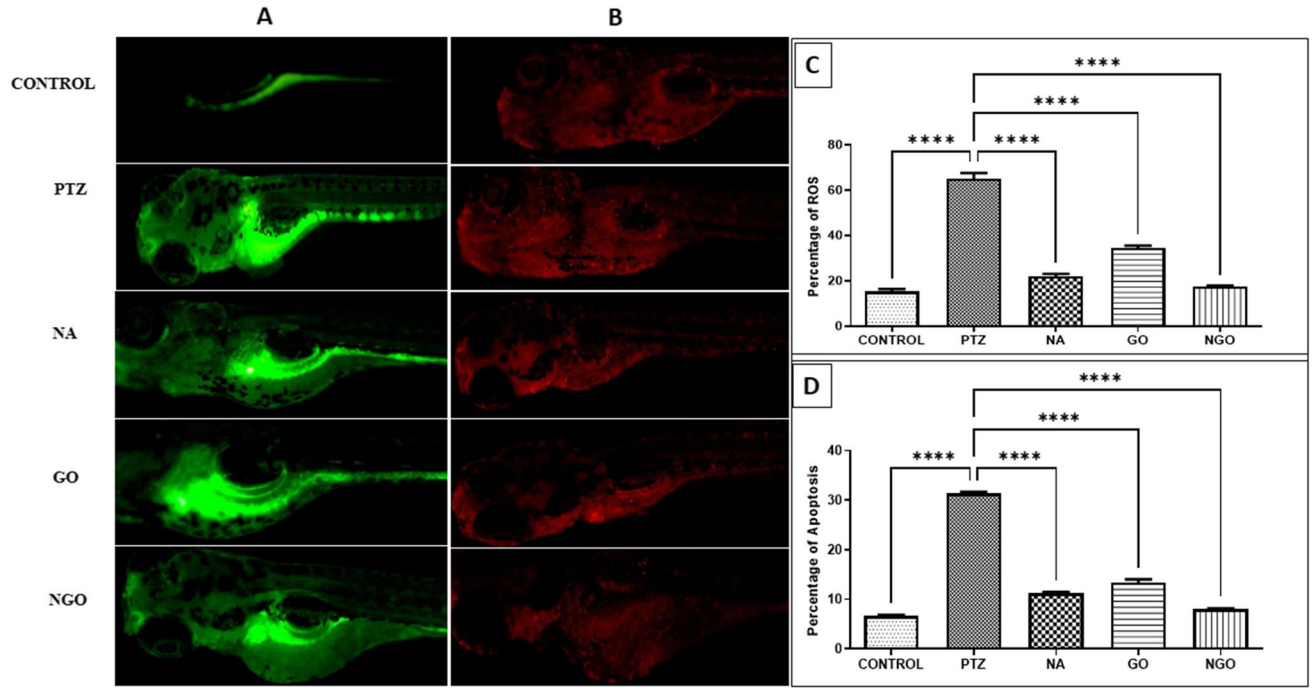

Fig. 5 In vivo fluorescent assays. (**a**) Images of zebrafish larvae stained with DCFDA fluorescent dye. The resultant green fluorescent observed represents the presence of ROS in the body of zebrafish larvae. (**b**) Cell apoptosis (red dots) in zebrafish larvae observed under the fluorescent microscope using acridine orange stain. (**c**) The percentage of ROS in larvae was quantified and plotted based on the fluorescent intensity using ImageJ software. (**d**) The percentage of apoptosis was calculated using ImageJ software. Control represents untreated larvae, PTZ represents Pentylenetetrazole, NA represents naringenin, GO represents graphene oxide, and NGO represents naringenin-graphene oxide nanoparticle-treated larvae. Graphs represent data from three independent experiments analysed by two-way anova followed by Dunnett multiple comparisons. **** represents a significant difference $p < 0.0001$

the toxic effect of GO was suppressed in the fabricated NGO nanoparticles.

3.5 Effect of NGO on PTZ-induced intracellular ROS in zebrafish larvae

The results obtained through the DCFDA staining assay are shown in Fig. 4. The percentage of ROS produced in control larvae was 15.8 ± 2.4, whereas the ROS observed in PTZ-exposed larvae was $65.5 \pm 3.23\%$. On the other hand, the level of ROS obtained in NA, GO, and NGO-treated larvae was decreased to 22.3 ± 1.2, 64.4 ± 1.8, and $17.8 \pm 0.8\%$, respectively. The strength of fluorescent intensity from DCFDA is directly proportional to the level of ROS present in the host. Hence, from the results, it is clear that PTZ exposure has induced the production of excess ROS in zebrafish larvae. Similarly, GO pre-treated larvae also showed a high intensity of green fluorescence, indicating that either GO has no effect on PTZ-induced ROS production or GO itself induces ROS production in zebrafish larvae. This was made evident in an earlier study [36, 37], which showed that graphene materials produce cytotoxicity by inducing ROS production. On the contrary, the results from NA and NGO pre-treated larvae showed a decrease in the ROS level after the PTZ-induced stress. Additionally, the level of ROS produced in NGO-pretreated larvae was less compared with NA and GO-pretreated larvae. This indicates the enhanced potential of fabricated nanoparticles in scavenging intracellular ROS.

3.6 Effect of NGO on PTZ-induced apoptosis

The results from the acridine orange stain show that, during 15 mM PTZ exposure, the percentage of cells undergoing apoptosis was 30.8 ± 0.7. In contrast, this percentage dropped to 11.2 ± 0.3, 33.5 ± 1.3, and $8.02 \pm 0.41\%$ in zebrafish larvae pre-treated with NA and NGO, respectively. The resultant images obtained through fluorescent observation and the intensity quantification graph are shown in Fig. 5. Excess of ROS leads cells to undergo stress-mediated apoptosis via a Caspase-dependent pathway. Our results from acridine orange staining showed a

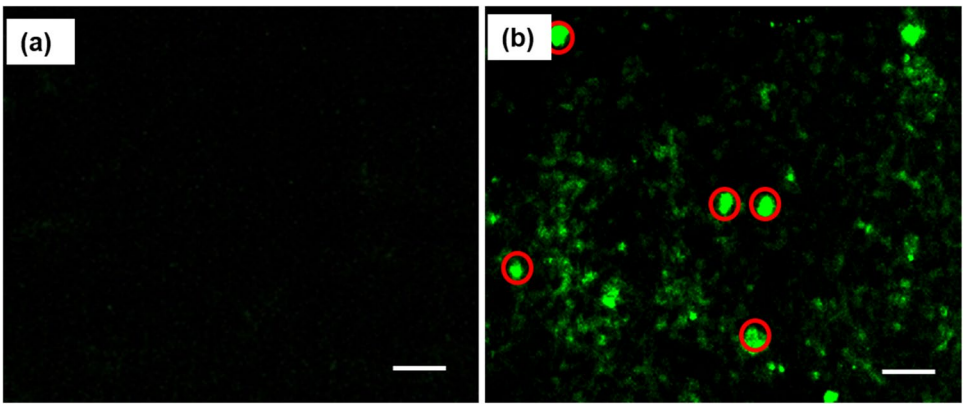

Fig. 6 Localisation of FITC-tagged NGO nanoparticles. The image represents the tissue sections of an adult zebrafish brain observed under a green channel of the fluorescent microscope. (**a**) Brain tissue of zebrafish from the control group injected with 1X PBS (without FITC-tag). (**b**) Green fluorescence emitted from tissue sectioned from zebrafish injected with FITC-tagged NGO nanoparticles (highlighted in red). Scale = 5 µm

high percentage of apoptotic cells in PTZ and GO pre-treated groups. On the contrary, the results from NA and NGO pre-treated larvae showed significantly less percentage of apoptotic cells compared with larvae exposed only to PTZ. This decrease in cellular apoptosis might be due to the reduced ROS level discussed earlier in the DCFDA assay [38].

3.7 Localisation of NGO in zebrafish brain

The fluorescent emissions from FITC tagged with NGO were observed and photographed to determine the localisation of drug in the zebrafish brain (Fig. 6). The resultant fluorescent images showed the presence of green fluorescent dots throughout the brain tissue of adult zebrafish, which

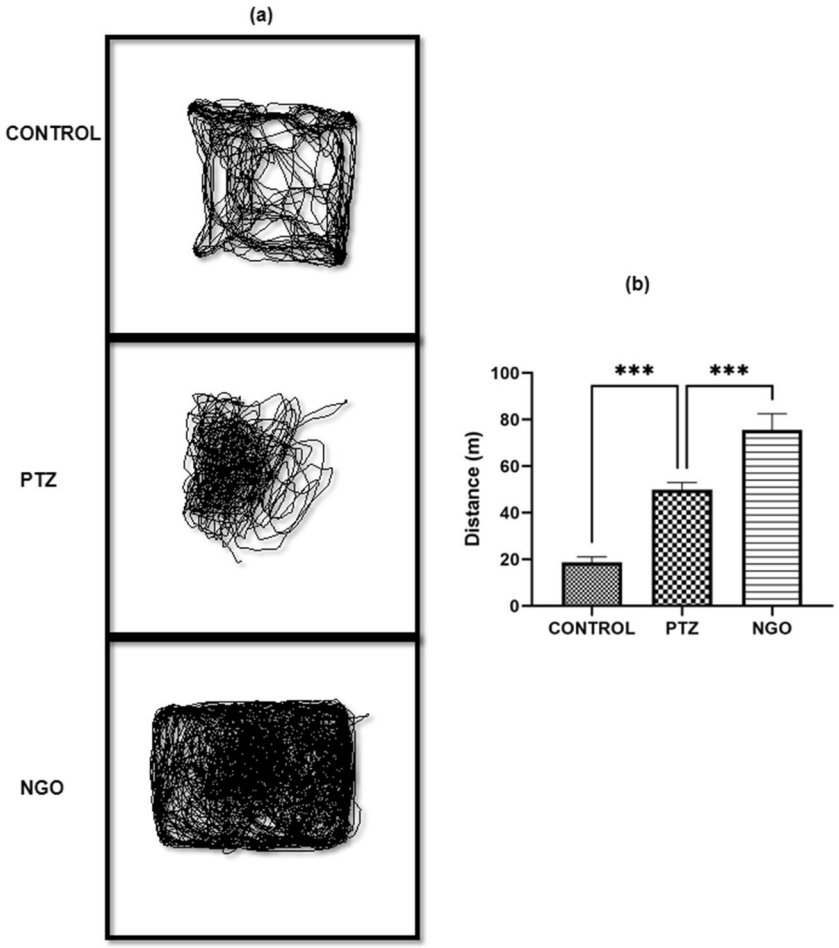

Fig. 7 Behavioural analysis in zebrafish using novel tank test. (**a**) The movement of adult zebrafish injected with 1X PBS (control), PTZ and NGO was tracked using UMATracker. The zebrafish in the control group explored all the areas novel tank, whereas the PTZ-exposed zebrafish failed to explore all edges of the novel tank and also showed swirl-like (convulsant) behaviour. The zebrafish pre-treated with NGO explored the novel tank as observed by the fish from the control group. (**b**) The distance moved by zebrafish from each group was calculated and plotted as a graph. The graph represents the distance travelled by adult zebrafish in control, PTZ and NGO groups for the time period of 5 min. *** represents a significant difference $p < 0.001$

represents the successful localisation of NGO nanoparticles in brain. The previous reports proved that, at lower concentrations, the uptake of anionic nanoparticles through BBB was higher compared with cationic or neutral nanoparticles [39]. In this study, FITC-tagged NGO was found localised in sectioned tissues of zebrafish brains, indicating that the anionic nature of fabricated nanoparticles proved its efficacy in passing through the BBB.

3.8 Locomotion analysis of adult zebrafish

The locomotion analysis on adult zebrafish indicates that the adult zebrafish exposed to 15 mM PTZ solution showed confused and swirl-like behaviour. Additionally, a novel tank assay showed that PTZ-exposed zebrafish failed to explore all the areas of the tank compared with the fish from the control group (Fig. 7). Similar behavioural result in PTZ-exposed zebrafish was previously reported [40]. On the contrary, NGO-injected adults explored all the areas of the novel tank similar to the fish from the control group. However, NGO-injected fish showed hyperactive movement and moved up to 76.3 ± 8.1 m. In contrast, fish from the control and PTZ group moved 18.7 ± 2.4 and 49.5 ± 3.7 m, respectively. From the results of behavioural analysis, we hypothesise that pre-treatment of NGO has prevented convulsant behaviour in adult zebrafish. Being a sensitive environment to oxidative stresses, the brain requires the addition of external antioxidants to manage the oxidative stressors and its related damages. There are several hypotheses that suggest the use of antioxidants to prevent the onset of epilepsy by mitigating neuronal damage by free radicals [41]. A study by Fontana et al. [42] reported the antioxidant and anticonvulsant effect of Taurine in the zebrafish model. In the current study, we found similar results which support the hypothesis that NGO nanoparticle prevented convulsant behaviour in zebrafish by mitigating the oxidative stress induced by PTZ exposure.

4 Conclusion

In this study, for the first time, we fabricated nanoparticles by combining naringenin and graphene oxide and characterised their physiochemical, morphological and biological properties. We have found that fabricated NGO showed enhanced antioxidant activity in vitro on comparing with free naringenin. The results from developmental toxicity analysis indicate that the fabricated nanoparticle was non-toxic and additionally, we found that the toxic effect of GO was suppressed while preparing a nanocomposite. Our results also provided pieces of evidence that NGO reduced the levels of ROS and subsequent apoptosis induced by PTZ in zebrafish larvae. Behavioural analysis with adult zebrafish proved that NGO has the potential to reduce the convulsant effect induced by kindling through PTZ exposure. Hence, we conclude that NGO can be taken to further pharmacological studies to develop as an efficient anticonvulsant agent.

Acknowledgement The authors express their sincere appreciation to the Researchers Supporting Project Number (RSP2023R414), King Saud University, Riyadh, Saudi Arabia.

Author contribution Raghul Murugan: Conceptualization, Methodology, Formal analysis, Investigation, Visualisation, Writing—Original Draft, Writing—Review & Editing. G. Mukesh: Methodology, Formal analysis, Investigation, Visualisation, Writing—Review & Editing. B. Haridevamuthu: Methodology, Formal analysis, Investigation, Writing—Review & Editing. P. Snega Priya: Methodology, Formal analysis, Investigation. Raman Pachaiappan, Bader O. Almutairi, Selvaraj Arokiyaraj: Methodology, Formal analysis, Investigation, Resources. Ajay Guru, Jesu Arockiaraj: Conceptualisation, Methodology, Funding acquisition, Formal analysis, Supervision, Writing – review & editing, Project administration.

Data availability Data will be made available on reasonable request.

Declarations

Ethical approval The experiments were performed following the guidelines of the institutional animal ethical approval (No. SAF/IAEC/211215/004).

Competing interests The authors declare no competing interests.

References

1. Moshé SL, Perucca E, Ryvlin P, Tomson T (2015) Epilepsy: new advances. Lancet 385:884–898. https://doi.org/10.1016/S0140-6736(14)60456-6
2. Trinka E, Kwan P, Lee B, Dash A (2019) Epilepsy in Asia: disease burden, management barriers, and challenges. Epilepsia 60:7–21. https://doi.org/10.1111/epi.14458
3. Kumar M, Kumar P (2017) Protective effect of spermine against pentylenetetrazole kindling epilepsy induced comorbidities in mice. Neurosci Res 120:8–17. https://doi.org/10.1016/j.neures.2017.02.003
4. Aguiar CCT, Almeida AB, Araújo PVP et al (2012) Oxidative stress and epilepsy: literature review. Oxid Med Cell Longev 2012:1–12. https://doi.org/10.1155/2012/795259
5. Malinska D, Kulawiak B, Kudin AP et al (2010) Complex III-dependent superoxide production of brain mitochondria contributes to seizure-related ROS formation. Biochim Biophys Acta - Bioenerg 1797:1163–1170. https://doi.org/10.1016/j.bbabio.2010.03.001
6. Zhu X, Dong J, Shen K et al (2015) NMDA receptor NR2B subunits contribute to PTZ-kindling-induced hippocampal astrocytosis and oxidative stress. Brain Res Bull 114:70–78. https://doi.org/10.1016/j.brainresbull.2015.04.002

7. Kovács R, Rabanus A, Otáhal J et al (2009) Endogenous nitric oxide is a key promoting factor for initiation of seizure-like events in hippocampal and entorhinal cortex slices. J Neurosci 29:8565–8577. https://doi.org/10.1523/JNEUROSCI.5698-08.2009
8. Zhu X, Dong J, Han B et al (2017) Neuronal nitric oxide synthase contributes to PTZ kindling epilepsy-induced hippocampal endoplasmic reticulum stress and oxidative damage. Front Cell Neurosci 11:1–16. https://doi.org/10.3389/fncel.2017.00377
9. Vauzour D, Vafeiadou K, Rodriguez-Mateos A et al (2008) The neuroprotective potential of flavonoids: a multiplicity of effects. Genes Nutr 3:115–126. https://doi.org/10.1007/s12263-008-0091-4
10. Hassan HM, Elnagar MR, Abdelrazik E et al (2022) Neuroprotective effect of naringin against cerebellar changes in Alzheimer's disease through modulation of autophagy, oxidative stress and tau expression: an experimental study. Front Neuroanat 16:1012422. https://doi.org/10.3389/fnana.2022.1012422
11. Pardridge WM (2012) Drug transport across the blood–brain barrier. J Cereb Blood Flow Metab 32:1959–1972. https://doi.org/10.1038/jcbfm.2012.126
12. Ceña V, Játiva P (2018) Nanoparticle crossing of blood–brain barrier: a road to new therapeutic approaches to central nervous system diseases. Nanomedicine 13:1513–1516. https://doi.org/10.2217/nnm-2018-0139
13. Tabish TA, Narayan RJ (2021) Crossing the blood–brain barrier with graphene nanostructures. Mater Today 51:393–401. https://doi.org/10.1016/j.mattod.2021.08.013
14. Tapeinos C (2021) Graphene-based nanotechnology in neurodegenerative disorders. Adv NanoBiomed Res 1:2000059. https://doi.org/10.1002/anbr.202000059
15. Vinodhkumar G, Ramya R, Vimalan M et al (2018) Reduced graphene oxide based on simultaneous detection of neurotransmitters. Prog Chem Biochem Res 1:40–49. https://doi.org/10.29088/SAMI/PCBR.2018.1.4049
16. Bellet P, Gasparotto M, Pressi S et al (2021) Graphene-based scaffolds for regenerative medicine. Nanomaterials 11:404. https://doi.org/10.3390/nano11020404
17. Rahmanian N, Hamishehkar H, Dolatabadi JEN, Arsalani N (2014) Nano graphene oxide: a novel carrier for oral delivery of flavonoids. Colloids Surf B Biointerfaces 123:331–338. https://doi.org/10.1016/j.colsurfb.2014.09.036
18. Priya PS, Vaishnavi S, Pavithra V et al (2023) Graphene oxide decorated daidzein as an oral drug to ameliorate the oxidative stress and glucocorticoid-induced osteoporosis in vivo zebrafish model. J Drug Deliv Sci Technol 81:104278. https://doi.org/10.1016/j.jddst.2023.104278
19. Rueden CT, Schindelin J, Hiner MC et al (2017) Image J2: ImageJ for the next generation of scientific image data. BMC Bioinformatics 18:529. https://doi.org/10.1186/s12859-017-1934-z
20. Prabha N, Guru A, Harikrishnan R et al (2022) Neuroprotective and antioxidant capability of RW20 peptide from histone acetyltransferases caused by oxidative stress-induced neurotoxicity in in vivo zebrafish larval model. J King Saud Univ - Sci 34:101861. https://doi.org/10.1016/j.jksus.2022.101861
21. Guru A, Velayutham M, Arockiaraj J (2022) Lipid-lowering and antioxidant activity of RF13 peptide from vacuolar protein sorting-associated protein 26B (VPS26B) by modulating lipid metabolism and oxidative stress in HFD induced obesity in zebrafish larvae. Int J Pept Res Ther 28:74. https://doi.org/10.1007/s10989-022-10376-3
22. Pekarova M, Kralova J, Kubala L et al (2009) Carvedilol and adrenergic agonists suppress the lipopolysaccharide-induced no production in raw 264.7 macrophages via the adrenergic receptors. J Physiol Pharmacol 60:143–150
23. Haridevamuthu B, Manjunathan T, Guru A et al (2022) Hydroxyl containing benzo[b]thiophene analogs mitigates the acrylamide induced oxidative stress in the zebrafish larvae by stabilising the glutathione redox cycle. Life Sci 298:120507. https://doi.org/10.1016/j.lfs.2022.120507
24. Sudhakaran G, Prathap P, Guru A et al (2022) Reverse pharmacology of Nimbin-N2 attenuates alcoholic liver injury and promotes the hepatoprotective dual role of improving lipid metabolism and downregulating the levels of inflammatory cytokines in zebrafish larval model. Mol Cell Biochem 477:2387–2401. https://doi.org/10.1007/s11010-022-04448-7
25. Sarkar P, Guru A, Raju SV et al (2021) GP13, an Arthrospira platensis cysteine desulfurase-derived peptide, suppresses oxidative stress and reduces apoptosis in human leucocytes and zebrafish (Danio rerio) embryo via attenuated caspase-3 expression. J King Saud Univ Sci 33:101665. https://doi.org/10.1016/j.jksus.2021.101665
26. Sari MM (2013) Fluorescein isothiocyanate conjugated graphene oxide for detection of dopamine. Mater Chem Phys 138:843–849. https://doi.org/10.1016/j.matchemphys.2012.12.069
27. Yamanaka O, Takeuchi R (2018) UMATracker: an intuitive image-based tracking platform. J Exp Biol 221:1–5. https://doi.org/10.1242/jeb.182469
28. Ferrari M, Downing G (2005) Medical Nanotechnology. BioDrugs 19:203–210. https://doi.org/10.2165/00063030-200519040-00001
29. Ahmad A, Fauzia E, Kumar M et al (2019) Gelatin-coated polycaprolactone nanoparticle-mediated naringenin delivery rescue human mesenchymal stem cells from oxygen glucose deprivation-induced inflammatory stress. ACS Biomater Sci Eng 5:683–695. https://doi.org/10.1021/acsbiomaterials.8b01081
30. Krishnakumar N, Sulfikkarali N, RajendraPrasad N, Karthikeyan S (2011) Enhanced anticancer activity of naringenin-loaded nanoparticles in human cervical (HeLa) cancer cells. Biomed Prev Nutr 1:223–231. https://doi.org/10.1016/j.bionut.2011.09.003
31. Jacox ME (2003) Vibrational and electronic energy levels of polyatomic transient molecules. Supplement B. J Phys Chem Ref Data 32:1–441. https://doi.org/10.1063/1.1497629
32. Sengupta I, Kumar SSS, Gupta K, Chakraborty S (2021) In-vitro release study through novel graphene oxide aided alginate based pH-sensitive drug carrier for gastrointestinal tract. Mater Today Commun 26:101737. https://doi.org/10.1016/j.mtcomm.2020.101737
33. Francenia Santos-Sánchez N, Salas-Coronado R, Villanueva-Cañongo C, Hernández-Carlos B (2019) Antioxidant compounds and their antioxidant mechanism. Antioxidants 1–28 https://doi.org/10.5772/intechopen.85270
34. Hersh AM, Alomari S, Tyler BM (2022) Crossing the blood-brain barrier: advances in nanoparticle technology for drug delivery in neuro-oncology. Int J Mol Sci 23:4153. https://doi.org/10.3390/ijms23084153
35. Zhang X, Zhou Q, Zou W, Hu X (2017) Molecular mechanisms of developmental toxicity induced by graphene oxide at predicted environmental concentrations. Environ Sci Technol 51:7861–7871. https://doi.org/10.1021/acs.est.7b01922
36. Cebadero-Domínguez O, Ferrández-Gómez B, Sánchez-Ballester S et al (2022) In vitro toxicity evaluation of graphene oxide and reduced graphene oxide on Caco-2 cells. Toxicol Rep 9:1130–1138. https://doi.org/10.1016/j.toxrep.2022.05.010
37. Zhang J, Cao H-Y, Wang J-Q, et al (2021) Graphene oxide and reduced graphene oxide exhibit cardiotoxicity through the regulation of lipid peroxidation, oxidative stress, and mitochondrial dysfunction. Front Cell Dev Biol 9 https://doi.org/10.3389/fcell.2021.616888
38. Lim YJ, Kim JH, Pan JH et al (2018) Naringin protects pancreatic β-cells against oxidative stress-induced apoptosis by inhibiting

both intrinsic and extrinsic pathways in insulin-deficient diabetic mice. Mol Nutr Food Res 62:1–47. https://doi.org/10.1002/mnfr.201700810

39. Lockman PR, Koziara JM, Mumper RJ, Allen D (2004) Nanoparticle surface charges alter blood-brain barrier integrity and permeability. J Drug Target 12:635–641. https://doi.org/10.1080/10611860400015936
40. Myren-Svelstad S, Jamali A, Ophus SS et al (2022) Elevated photic response is followed by a rapid decay and depressed state in ictogenic networks. Epilepsia 63:2543–2560. https://doi.org/10.1111/epi.17380
41. Martinc B, Grabnar I, Vovk T (2015) Antioxidants as a preventive treatment for epileptic process: a review of the current status. Curr Neuropharmacol 12:527–550. https://doi.org/10.2174/1570159X12666140923205715
42. Fontana BD, Ziani PR, Canzian J et al (2019) Taurine protects from pentylenetetrazole-induced behavioral and neurochemical changes in zebrafish. Mol Neurobiol 56:583–594. https://doi.org/10.1007/s12035-018-1107-8